NUKLEONIKA 2017;62(3):229–234
doi: 10.1515/nuka-2017-0033

ORIGINAL PAPER

Deconvolution of alpha spectra from air filters applied for measurements of the short-lived radon progeny concentration

Krystian Skubacz

Abstract. The paper contains a description of a method for the analysis of the complex alpha spectra generated during the measurement of the activity of filters outside of a vacuum chamber under environmental conditions. The peaks corresponding to the energies of alpha particles emitted by the specific isotopes are particularly large on the low-energy side of the peak maximum, and the energy resolution strongly depended on the applied filters. The analysis was based on the non-linear regression to a function designed for four, six and eight parameters. Satisfactory results were obtained for each of these functions, and the best-fitting results were achieved for the eight-parameter function. In addition, the uncertainties related to the estimated parameters, as well as the signals corresponding to functions that describe the shape of the energy peak, have been evaluated. There are also examples of the implementation of the method with respect to short-lived radon progeny and thoron decay products.

Keywords: alpha spectroscopy • ambient pressure • spectrum analysis • non-linear regression • radon progeny • thoron progeny

Introduction

In many cases, the spectrometric measurements of radionuclides collected on filters must be performed outside of a vacuum chamber, at or close to atmospheric pressure. That is the case with the analysis carried out in air-monitoring stations [1, 2], as well as with the measurements of the concentration of short-lived radon decay products with impactors [3, 4] and screen diffusion batteries [5–8]. In such cases, the peaks corresponding to specific radionuclides are much wider, particularly on the low-energy side of the peak, and overlap each other. As follows, it becomes necessary to precisely separate the peaks related to the individual radionuclide. An accurate spectrum analysis becomes particularly important when differential measurements are performed, like in the case of the evaluation of the unattached fraction of short-lived radon decay products by the parallel activity measurement of an open filter and filter shielded by a diffusion screen [8]. Such an analysis can be carried out through the use of non-linear regression and appropriate functions that allow for an accurate representation of the peak shape. The developed method made it possible to achieve valid results with functions dependent on four, six and eight parameters.

Pöllänen and Siiskonen [9] performed detailed deconvolution of such alpha-energy spectra related

K. Skubacz
Central Mining Institute,
Silesian Centre for Environmental Radioactivity (BCR),
Plac Gwarków 1, 40-166 Katowice, Poland,
Tel.: +48 32 259 2816, Fax: +48 32 259 2295,
E-mail: kskubacz@gig.eu

Received: 3 June 2016
Accepted: 16 May 2017

to short-lived radon progeny collected on the air filters that were placed after exposition inside a vacuum chamber to do data acquisition. In most cases, however, there is no possibility to use a vacuum chamber when performing environmental measurements and they have to be done at ambient pressure. During the unfolding of spectra, they applied Gaussian functions to fit it to the specific energy of alpha particles. In this paper, more complex functions were found and used for better fitting, especially in the region of peak widening and tailing on the low-energy side. New software was necessary to analyse the spectrum using these functions, evaluate the effectiveness of the entire minimizing procedure and calculate all quantities that relate exactly to these functions. Also tested was the effectiveness of the different methods applied to find the minimum value.

This method was applied to unfold spectra obtained during measurements of the unattached fraction of the short-lived radon progeny. The unattached fraction is for the most part below 10 percent, higher in the clean air and lower in the dusty atmosphere. This results in a rather large uncertainty when comparing spectra related to the open-face filter and filter shielded by a diffusion battery screen used to remove unattached particles from the air stream. Detailed spectrum analysis can reduce uncertainty.

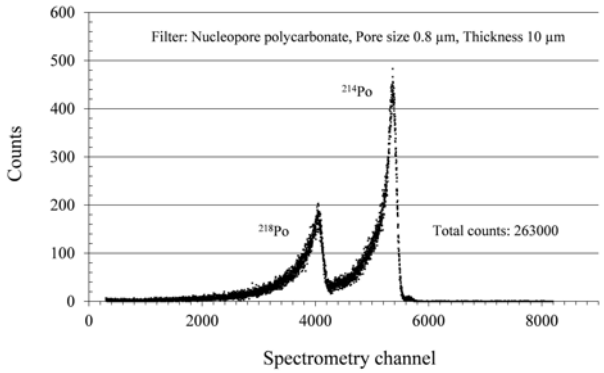

Fig. 1. Spectrum generated by ^{214}Po and ^{218}Po isotopes collected on the Nucleopore Polycarbonate filter with pore size of 0.8 μm.

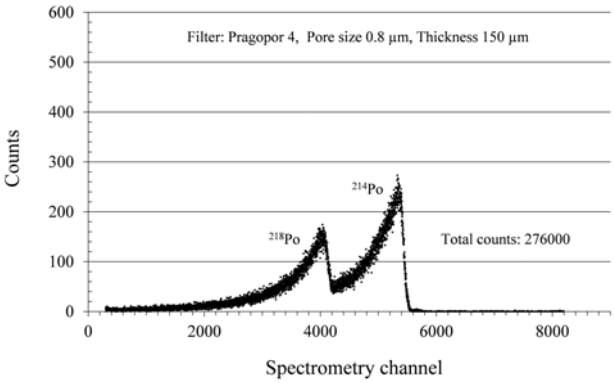

Fig. 2. Spectrum generated by ^{214}Po and ^{218}Po isotopes collected on the Pragopor 4 filter with pore size of 0.8 μm.

Materials and measurement method

Non-linear regression was used to analyse the alpha radiation spectra of isotopes collected by Nucleopore Polycarbonate filters (Costar Corporation, USA) with a thickness of 10 μm and pore diameter of 0.8 μm, or Pragopor 4 filters composed of nitrocellulose (Pragochema, Czech Republic) with a thickness of 150 μm and pore diameter of 0.85 μm. In addition to thickness, the filters differ in the arrangement and orientation of their pores. The Nucleopore Polycarbonate filters have pores that are regular in shape, passing through and oriented perpendicular to the surface. In turn, the orientation of the pores in the Pragopor 4 filter is disordered, and the air travels a longer distance through its structure. This improves filtration efficiency, but on the other hand, it reduces the energy resolution. For such filters, the alpha source becomes considerably more than 1 μm thick, causing notable peak widening and tailing, and difficulties in the analysis [9, 10].

The spectra that correspond to the both filters can be compared in Figs. 1 and 2. The short-lived radon progeny were collected on the filters in the radon chamber of 17 m^3 volume at the same time, and the same condition such as sampling flow rate and sampling time. The number of total counts is nearly the same, but the energy resolution is considerably better for the Nucleopore Polycarbonate filter (Fig. 1) than for the Pragopor 4 filter (Fig. 2).

The alpha activity of the filters was measured by means of an ULTRACAM solid-state detector with an active surface of 1700 mm^2. Its surface is covered with a 0.5 μm aluminium and 1 μm emulsion layer, which is the total equivalent of a 1 μm aluminium layer for alpha particles. As a result, the energy resolution of the detector is worse compared to conventional alpha detectors, but it better suited for use in harsh environmental conditions. The distance between the filters and the detector surface was 2 mm, and the BIAS voltage equals to 30 V.

Algorithm

Spectrum analysis was performed using the regression method, according to which the value of a χ^2 expressed by the formula (1) is to be minimum:

$$\chi^2 = \sum_{i=1}^{N} \omega_i [y_i - F(x_i, p)]^2 \tag{1}$$

where x_i is the number of spectrometer channel, y_i the number of counts in the channel x_i, $\omega_i = 1/y_i$ the weight indicating the credibility of this result, N the number of spectrometer channels and p the set of parameters that must be optimized to find the minimum of χ^2 function. It is a problem of non-linear regression due to the chosen form of the F functions. If the analysis includes M independent alpha energy peaks, the function F is the sum of functions representing the M independent energy peaks:

$$F(x_i, p) = F_1(x_i, p^{(1)}) + \ldots + F_M(x_i, p^{(M)}) \tag{2}$$

Three functions have been designed to finally solve this problem and for comparison with each other. They depend on four, six or eight parameters, are partially based on the Gaussian function defined commonly by three parameters (p_1, p_2, and p_3 as in the formulas (3)–(5)) and can be successfully applied to obtain, as a result of the minimization process, a good mathematical representation of the measured results. The spectrum variation on the low-energy side and the greater distance from the peak maximum are not so violent. That is why slowly changing components were added to the Gaussian function in the following formulas:

– Four-parameter function

$$(3)\qquad F(x,p)=\begin{cases} p_1 e^{\frac{2xp_4+p_4^2-2p_3p_4}{2p_2}} & x\le p_3-p_4 \\ p_1 e^{-\frac{(x-p_3)^2}{2p_2}} & x>p_3-p_4 \end{cases}$$

– Six-parameter function

$$(4)\quad F(x,p)=\begin{cases} p_1 e^{\frac{2p_4p_5+p_4^2-2p_3p_4}{2p_2}} e^{p_6(x-p_5)} & x\le p_5 \\ p_1 e^{\frac{2xp_4+p_4^2-2p_3p_4}{2p_2}} & p_5<x\le p_3-p_4 \\ p_1 e^{-\frac{(x-p_3)^2}{2p_2}} & x>p_3-p_4 \end{cases}$$

– Eight-parameter function

$$(5)\ F(x,p)=\begin{cases} p_1 e^{\frac{2p_4p_5+p_4^2-2p_3p_4}{2p_2}} e^{p_6(p_7-p_5)} e^{p_8(x-p_7)} & x\le p_7 \\ p_1 e^{\frac{2p_4p_5+p_4^2-2p_3p_4}{2p_2}} e^{p_6(x-p_5)} & p_7<x\le p_5 \\ p_1 e^{\frac{2xp_4+p_4^2-2p_3p_4}{2p_2}} & p_5<x\le p_3-p_4 \\ p_1 e^{-\frac{(x-p_3)^2}{2p_2}} & x>p_3-p_4 \end{cases}$$

Parameters such as p_3, p_4, p_5 and p_7 merely divide the total channel range into smaller parts, and the functions were designed to be continuous at the ends of these specified intervals. The optimized χ^2 function is differentiable for such selection, and the gradient descent method can be used as an optimization algorithm. According to this procedure, the direction d should be found, which indicates the decline of the χ^2 function, and subsequently the value that defines the vector τd for which it takes a minimum. Such a step-by-step process allows for the calculation of a local minimum. Two methods known in statistics and designed to find the direction were tested. The first one is based on a gradient, and the second is the Newton's method on the Hessian matrix H_{jr}. The third method relies on the matrix M_{jr} constructed on the basis of weighing the values and derivatives of the F function. All of these methods are defined as follows:

$$(6)\ d_j=-\frac{\partial\chi^2}{\partial p_j},\ d_j=-\sum_{r=1}^{L}H_{jr}^{-1}\frac{\partial\chi^2}{\partial p_r},\ d_j=-\sum_{r=1}^{L}M_{jr}^{-1}\frac{\partial\chi^2}{\partial p_r},$$

$$H_{jr}=\frac{\partial^2\chi^2}{\partial p_j\partial p_r},\ M_{jr}=\sum_{k=1}^{N}\omega_k\frac{\partial^2F(x_k,\overline{p})}{\partial p_j\partial p_r},$$

$$j=1,\ \ldots,L$$

where L is the number of parameters that describe the function (3)–(5). Every such function with a particular set of parameters corresponds to a particular alpha peak generated by an isotope, and the appropriate values of these parameters should be found during the minimization procedure of the quantity (1). In turn, the H – H^{-1} or M – M^{-1} are inverse matrices. The best results were achieved using the H_{jr} matrix, the M_{jr} matrix or a combination of these methods. In turn, the τ number, which indicates the minimum along the evaluated direction, was estimated according to the golden section search method or quadratic interpolation method (gradient or non-gradient). Among these methods, the golden section search was most effective.

The relationship between the output parameters p_{jO} and input parameters p_{jI} after every minimizing operation can thus be expressed as

$$(7)\qquad p_{jO}=p_{jI}+\tau d_j$$

The optimization process was interrupted after some specified criteria reached the accepted value, but only when the condition $\chi^2(p_O) < N - L$ was satisfied. These criteria are defined as follows:

$$(8)\qquad \delta(\chi^2)=\frac{\left|\chi_I^2-\chi_O^2\right|}{\chi_I^2},\ \delta(p)=\sqrt{\sum_{j=1}^{L}(p_{jO}-p_{jI})^2},$$

$$\text{Norm}=\sqrt{\sum_{i=1}^{L}\left(\left(\frac{\partial\chi^2}{\partial p_i}\right)_{p=p_O}\right)^2}$$

The quality of optimization can also be assessed by estimation of uncertainties for the estimated final parameters:

$$(9)\qquad \sigma(p_{jO})=\sqrt{G_{jj}^{-1}},$$

$$G_{jr}=\sum_{k=1}^{N}\omega_k\left(\frac{\partial F(x_k,p)}{\partial p_j}\right)_{p=p_O}\left(\frac{\partial F(x_k,p)}{\partial p_r}\right)_{p=p_O}$$

In turn, the counts in the x_i channel relate to the particular radioisotope that have been calculated based on the optimized function, and the corresponding uncertainties are equal to:

$$(10)\qquad y_{Ri}=F(x_i,p_O),\quad \sigma(y_{Ri})=\sqrt{Y_{ii}^{-1}},$$

$$Y_{ij}^{-1}=\sum_{k=1}^{L}\sum_{r=1}^{L}\left(\frac{\partial F(x_i,p)}{\partial p_r}\right)_{p=p_O}\left(\frac{\partial F(x_j,p)}{\partial p_k}\right)_{p=p_O}\cdot G_{rk}^{-1}$$

Short-lived radon progeny and thoron decay products

The alpha energy peaks related to the short-lived radon progeny and thoron decay products col-

lected on a filter correspond to five isotopes: ^{218}Po (6.002 MeV), ^{214}Po (7.687 MeV), ^{216}Po (6.778 MeV), ^{212}Bi (6.051 and 6.090 MeV) and ^{212}Po (8.784 MeV). Taking the simple assumption that the measurement is carried out after the completion of air pumping, the contribution of ^{216}Po can be neglected. In this case, there are only three separate alpha peaks, because the energies of alpha particles emitted by ^{218}Po and ^{212}Bi practically do not differ: ^{218}Po + ^{212}Bi (1), ^{214}Po (2) and ^{212}Po (3). Therefore, the spectrum can be described by three functions and then the estimated number of counts in the x_i channel is equal to:

$$y_{Rij} = F_j(x_i, p_O^{(j)}) \tag{11}$$

j = 1,2,3 for ^{218}Po + ^{212}Bi, ^{214}Po, and ^{212}Po, respectively.

The ^{212}Bi decays with 36% probability into ^{208}Tl releasing the alpha particles with nearly the same energy as ^{218}Po (about 6 MeV), and in 64% cases into ^{212}Po, that emits alpha particles with the considerably different energy (about 8.8 MeV). Hence, taking into account this branching ratio of ^{212}Bi, the total number of counts corresponding to these radionuclides is

$$S_{^{218}\mathrm{Po}} = \sum_{i=1}^{N} y_{Ri1} - \varphi \sum_{i=1}^{N} y_{Ri3},\ S_{^{212}\mathrm{Bi}} = \varphi \sum_{i=1}^{N} y_{Ri3}, \tag{12}$$
$$S_{^{214}\mathrm{Po}} = \sum_{i=1}^{N} y_{Ri2},\ S_{^{212}\mathrm{Po}} = \sum_{i=1}^{N} y_{Ri3},\ \varphi = \frac{0.36}{0.64}$$

In order to compare the uncertainties corresponding to the measurement results and counts estimated on the basis of the optimized function F, the covariance should be additionally considered as in the following formulas:

$$\sigma_{Toti}^2 = \sigma_{1i}^2 + \sigma_{2i}^2 + \sigma_{3i}^2 + 2\,\mathrm{cov}_{12i} + 2\,\mathrm{cov}_{13i} + 2\,\mathrm{cov}_{23i}$$
$$\sigma_{ji}^2 = \sum_{k=1}^{L}\sum_{r=1}^{L}\left(\frac{\partial F_j(x_i, p^{(j)})}{\partial p_k}\right)_{p^{(j)}=p_o^{(j)}} \cdot \left(\frac{\partial F_j(x_i, p^{(j)})}{\partial p_r}\right)_{p^{(j)}=p_o^{(j)}} \cdot G_{kr}^{-1} \tag{13}$$
$$\mathrm{cov}_{jki} = \sum_{s=1}^{L}\sum_{r=1}^{L}\left(\frac{\partial F_j(x_i, p^{(j)})}{\partial p_s}\right)_{p^{(j)}=p_o^{(j)}} \cdot \left(\frac{\partial F_k(x_i, p^{(k)})}{\partial p_r}\right)_{p^{(k)}=p_o^{(k)}} \cdot G_{sr}^{-1}$$

Results

Table 1 shows the results of fitting the four-, six- and eight-parameter functions to the peak generated by the alpha particles released during ^{214}Po decay. Although all curves fit well to this peak, the best results were achieved for the eight-parameter function, which is precisely matched – even close to the maximum, where the number of counts varies strongly from channel to channel. The difference in quality can especially be observed in relation to the assessment of the energy resolution, commonly defined as full width at half maximum (FWHM), which was clearly underestimated for the four- and six-parameter functions. According to the example reported in Table 1, every minimizing process was completed successfully. The lowest χ^2 value, however, was achieved for the eight-parameter analysis, as was the case for nearly 60 other completed minimizing procedures. The difference between the measured results and the estimated counts is also the smallest and equals 1.6%. On the other hand, however, such an analysis requires more time in comparison to an optimization with a smaller number of free parameters. In this example, the uncertainties related to the estimated parameters according to formula (9) were 3% on average (0.1 to 8.4%). The lowest uncertainty always corresponded to the p_3 parameter that defines the maximum location, and the highest to the p_4 parameter.

Figures 3 and 4 show the results of optimization when applying two eight-parameter functions F_1 and F_2 for ^{214}Po and ^{218}Po isotopes collected in a filter. In Fig. 3, the sum of these functions has been compared with the acquired spectrum in the logarithmic scale. In turn, the separated peaks that correspond to the ^{214}Po and ^{218}Po isotopes are presented in Fig. 4. The residual expressed as difference between measured results and sum of the F_1 and F_2 functions is shown in the bottom panel of this figure. The difference is mainly due to statistical errors related to the acquired spectrum, and the relative difference between the total number of counts and sum of the analytical functions F_1 and F_2, is only 1.2% (Table 2). It should be noted, however, that a strong match was also obtained for six-parameter functions. The uncertainties evaluated according to the formula (9) were larger for the F_1 function than for the F_2 function: 0.2–33% compared to 0.04–10%. As in the case of the one-isotope-spectrum, the lowest

Table 1. Optimization of the χ^2 function for the four-, six-, and eight-parameter functions fitted for the spectrum generated by ^{214}Po

Quantity	Value		
	L = 4	L = 6	L = 8
χ^2	2 223 → 860	17 128 → 527	48 411 → 459
$P \pm \sigma(P)$		28 188 ± 168	
^{214}Po: $P_{R1} \pm \sigma(P_{R1})$	27 335 ± 13	27 676 ± 14	27 743 ± 18
$100\lvert P - P_{R1}\rvert/P$	3.0%	1.8%	1.6%
^{214}Po: FWHM	203 channels	177 channels	141 channels
$\delta(\chi^2)$	<0.001	<0.001	<0.001
$\delta(p)$	<0.01	<0.01	<0.01
Norm	0.01	166	0.04

uncertainty corresponded also to the p_3 and the highest to the p_4 parameter.

During the calibration of the alpha spectrometry system, cigarette smoke or aerosols generated from 1% NaCl water solution were applied. The energy resolution FWHM evaluated based on the analytical functions was about 600 and 410 keV for ^{218}Po and ^{214}Po respectively when applying the polycarbonate filters and smoke aerosols. In the case of water-based aerosol, the FWHM was equal to about 400 and 330 keV for the same isotopes. For nitrocellulose filters, the energy resolution was tens of percents worse (Figs. 1 and 2).

A software Regres was developed to fulfil all the tasks according to the described algorithm. The program was also verified with help of the Mathematica software by Wolfram Research, Inc., in relation to such calculated quantities as peak area corresponding to given alpha isotopes, χ^2 value, and uncertainties defined in the algorithm.

The software was designated especially to analyse the spectra generated by short-lived radon progeny and thoron progeny. The evaluation of the unattached fraction of the short-lived radon progeny using screen diffusion battery [7] has to be performed very carefully. That is because of low difference between signals related to the attached aerosols, and aerosols consisting of the unattached and attached fraction. The unattached fraction is mainly below 10 percent, higher in the clean air and lower in the dusty atmosphere. That results in rather large uncertainty. When comparing the results of minimizing procedure, the relative difference between measured results and a function describing the peaks, was twice as great for four-parameter function than for the eight-parameter function. That is only if the statistic was at the level presented in Figs. 3 and 4. Additionally, the evaluated energy resolution, which defines the basic capability of the spectrometry system, was also very different for these functions (Table 1) because the four-parameter function did not fit well to the peak shape in the region of its maximum.

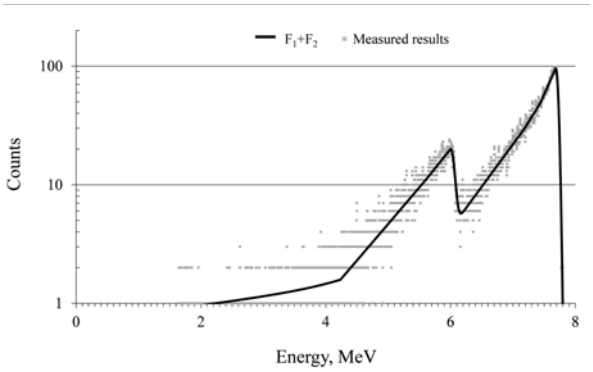

Fig. 3. Fitted and measured spectra generated by ^{214}Po and ^{218}Po collected on the Pragopor 4 filter.

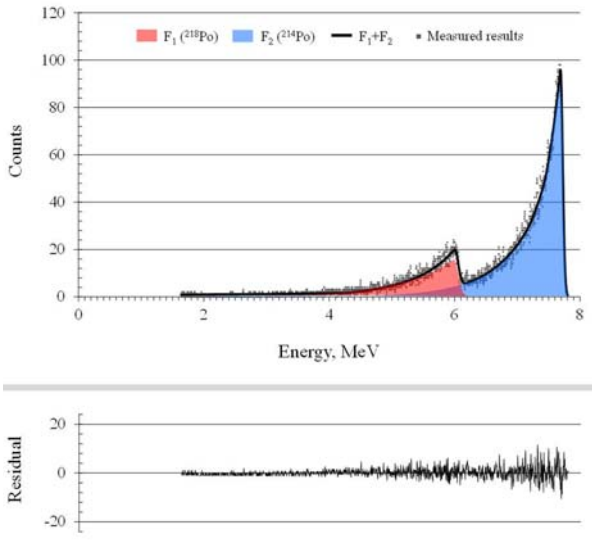

Fig. 4. Measured spectrum and fitted peaks corresponding to ^{214}Po and ^{218}Po collected on the Pragopor 4 filter. The residual on the bottom of the figure is the difference between measured results and sum of the F_1 and F_2 functions representing the fitted peaks.

Table 2. Minimization of the χ^2 function for the eight-parameter function fitted for spectrum generated by ^{218}Po and ^{214}Po

Quantity	Value
	$L = 8$
χ^2	130 534 → 710
$P \pm \sigma(P)$	29 403 ± 172
^{214}Po: $P_{R1} \pm \sigma(P_{R1})$	22 580 ± 18
^{218}Po: $P_{R2} \pm \sigma(P_{R2})$	6 465 ± 9
$100\lvert P - (P_{R1} + P_{R2})\rvert/P$	1.2%
^{214}Po: FWHM$_1$	137 channels
^{218}Po: FWHM$_2$	203 channels
$\delta(\chi^2)$	<0.001
$\delta(p)$	<0.01
Norm	247

The spectra generated by radon and thoron progeny can be analysed in most cases *a posteriori*. In emergency situation, however, the spectra have to be evaluated on-line and as soon as possible. That may be the case when smaller number of parameters is preferred but ultimately it depends on the capabilities of the computer system and needs of the users.

Conclusions

The method presented allows for the precise deconvolution of the overlapping alpha peaks and for an accurate assessment of counts corresponding to particular alpha-radioactive isotopes. The condition under which it is assumed that the fitting is satisfactory, $\chi^2(p_O) < N - L$, has been met for each of the defined functions. However, the best fit was always achieved for the eight-parameter function. Where the energy spectrum consisted of more than one peak, the six- and eight-parameter analysis achieved rather similar results. Subsequently, the six-parameter option can be considered a better solution, as it is less time-consuming.

Regardless of the fact that the software has been designated for the radon and thoron progeny, more complex spectra related also to other alpha emitters

collected on a filter can be analysed by taking into account the defined functions describing the corresponding peaks if only the energy resolution is not too low. However, evaluation of the concentration should be done separately and take into account estimated counts and other quantities that correspond to an isotope and measurement procedure such as half-life period, branching ratio, pumping time, flow rate during sampling, the interval of spectrum data acquisition, and counting efficiency.

Acknowledgment. This work was supported by the Ministry of Science and Higher Education of the Republic of Poland (Project no. 411/P05/97/13) and the Central Mining Institute, Katowice, Poland (CMI). The CMI has issued permission for the submission of this article for publication.

References

1. Pöllänen, R., & Siiskonen, T. (2006). High-resolution alpha spectrometry under field conditions – fast identification of alpha particle emitting radionuclides from air samples. *J. Env. Radioact*., *87*, 279–288.
2. Pöllänen, R., Peräjärvi, K., Siiskonen, T., & Turunen, J. (2013). In-situ alpha spectrometry from air filters at ambient air pressure. *Radiat. Meas*., *53/54*, 65–70.
3. Kesten, J., Butterweck, G., Porstendörfer, J., & Reineking, A. (1992). An online alpha impactor for short-lived radon daughter. *Aerosol Sci. Technol*., *18*, 156–164.
4. Porstendörfer, J., Zock, Ch., & Reineking, A. (2000). Aerosol size distribution of the radon progeny in outdoor air. *J. Environ. Radioact*., *51*, 37–48.
5. Cheng, Y. S., Su, Y. F., Newton, G. J., & Yeh, H. C. (1992). Use of a graded diffusion battery in measuring the activity size distributions of thoron progeny. *J. Aerosol Sci*., *23*(4), 361–372.
6. Reineking, A., Becker, K. H., & Porstendörfer, J. (1988). Measurements of the activity size distributions of the short-lived radon daughters in the indoor and outdoor environment. *Radiat. Prot. Dosim*., *24*, 245–250.
7. Reineking, A., & Porstendörfer, J. (1986). High-volume screen diffusion batteries and α-spectroscopy for measurement of the radon daughter activity size distributions in the daughter activity size distribution in the environment. *J. Aerosol Sci*., *17*(5), 873–879.
8. Reineking, A., & Porstendörfer, J. (1990). Unattached fraction of short-lived Rn decay products in indoor and outdoor environments: an improved single-screen method and results. *Health Phys*., *58*(6), 715–727.
9. Pöllänen, R., & Siiskonen, T. (2014). Unfolding alpha-particle energy spectrum from a membrane air filter containing radon progeny. *Radiat. Meas*., *70*, 15–20.
10. Lin, Z., Berne, A., Cummings, B., Filliben, J. J., & Inn, K. G. (2002). Competence of alpha spectrometry analysis algorithms used to resolve the ^{241}Am and ^{243}Am alpha peak overlap. *Appl. Radiat. Isot*., *56*, 57–63.